# Suppression of radiation loss in high kinetic inductance superconducting co-planar waveguides

Hahnle, S.; v. Marrewijk, N.; Endo, A.; Karatsu, K.; Thoen, D. J.; Murugesan, Vignesh; Baselmans, J. J. A.

**Important note**
To cite this publication, please use the final published version (if applicable).
Please check the document version above.

S. Hähnle (iD), N. v. Marrewijk, A. Endo, K. Karatsu, D. J. Thoen (iD), V. Murugesan, and J. J. A. Baselmans

View Online     Export Citation     CrossMark

## ARTICLES YOU MAY BE INTERESTED IN

Lock-in Amplifiers up to 600 MHz     Watch

# Suppression of radiation loss in high kinetic inductance superconducting co-planar waveguides

S. Hähnle,[1,2,a)] N. v. Marrewijk,[2] A. Endo,[2,3] K. Karatsu,[1,2] D. J. Thoen,[2] V. Murugesan,[1] and J. J. A. Baselmans[1,2]

## AFFILIATIONS

[1]SRON - Netherlands Institute for Space Research, Sorbonnelaan 2, 3584 CA Utrecht, The Netherlands
[2]Department of Microelectronics, Faculty of Electrical Engineering, Mathematics and Computer Science (EEMCS),
  Delft University of Technology, Mekelweg 4, 2628 CD Delft, The Netherlands
[3]Kavli Institute of NanoScience, Faculty of Applied Sciences, Delft University of Technology, Delft, The Netherlands

[a)]Author to whom correspondence should be addressed: s.haehnle@sron.nl

## ABSTRACT

We present a lab-on-chip technique to measure the very low losses in superconducting transmission lines at (sub-) mm wavelengths. The chips consist of a 100 nm-thick NbTiN Co-planar Waveguide (CPW) Fabry–Pérot (FP) resonator, coupled, on one side, to an antenna and, on the other side, to a Microwave Kinetic Inductance detector. Using a single frequency radiation source allows us to measure the frequency response of the FP around 350 GHz and deduce its losses. We show that the loss is dominated by radiation loss inside the CPW line that forms the FP and that it decreases with the decreasing linewidth and increasing kinetic inductance as expected. The results can be quantitatively understood using SONNET simulations. The lowest loss is observed for a CPW with a total width of 6 $\mu$m and corresponds to a Q-factor of $\approx$15 000.

*Published under license by AIP Publishing.* https://doi.org/10.1063/5.0005047

Superconducting transmission lines, such as co-planar waveguides (CPWs) or microstrips, are increasingly prevalent for cryogenic high-frequency applications above 100 GHz, such as on-chip spectrometers,[1–3] phased array antennas,[4] and kinetic inductance parametric amplifiers.[5] These applications require ultralow-loss transmission lines with a loss tangent of $\tan \delta \lesssim 10^{-3}$ and lengths above 100$\lambda$, either as an integral part of the circuit in kinetic inductance parametric amplifiers or phased array antennas or as a connecting element in on-chip spectrometers. Microstrip losses in this frequency range down to $\tan \delta = 2 \times 10^{3}$ have been measured previously.[6] Here, we focus on losses in CPWs. CPW lines have an advantage over microstrip lines in that they do not require a deposited dielectric, which is a source of loss, decoherence, and noise. However, CPWs are open structures and can radiate power, which are a source of loss and increase cross coupling to neighboring lines. The dominant radiation loss mechanism is the so-called leaky mode, which is present if the phase velocity in the line exceeds the phase velocity in the substrate. For microwave applications, this can be controlled by reducing the linewidth, but this becomes increasingly impractical at mm- and sub-millimeter wavelengths. In superconducting lines, the phase velocity is

reduced due to kinetic inductance, which, in principle, allows us to create a line with a phase velocity below the substrate phase velocity, thereby eliminating the leaky mode radiation and creating ultralow-loss transmission lines at frequencies exceeding hundreds of GHz. Dielectric losses in microstrips at frequencies up to 100 GHz have been measured previously.[6] In this paper, we demonstrate lab-on-chip loss measurements of superconducting NbTiN CPW Fabry–Pérot resonators around 350 GHz. We show that the radiation loss can be reduced and even virtually eliminated by reducing the phase velocity, which is accomplished by narrowing the CPW line to a total width of $\lesssim$6 $\mu$m.

The effective dielectric constant of a transmission line using a perfect electric conductor (PEC) is given by

$$\varepsilon_{eff} = c^2 LC, \quad (1)$$

where $c$ is the speed of light and $L$ and $C$ are the transmission line inductance and capacitance per unit length, respectively. In a CPW as shown in Fig. 1, this can be approximated by

$$\varepsilon_{eff} \approx \frac{\varepsilon_r + 1}{2}, \quad (2)$$
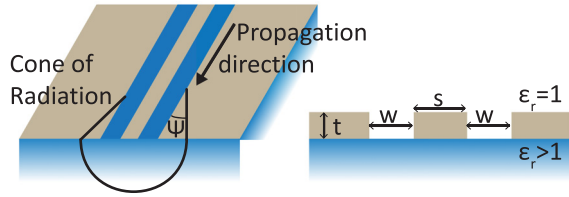
**FIG. 1.** (a) CPW geometry. (b) Cone of radiation emitted along the propagation direction of the CPW mode, with radiation angle $\Psi$.

with the dielectric constant of the substrate $\varepsilon_r$. The phase velocity $v_{ph} = \frac{c}{\sqrt{\varepsilon_{eff}}}$ in the guided CPW mode is, therefore, faster than that in the substrate. This creates a shockwave in the substrate, leading to a radiation cone characterized by the radiation angle $\Psi$ (see Fig. 1). The frequency-dependent loss factor $\alpha$ at high frequencies due to this shockwave has been derived by Frankel et al.[7] from the electric and magnetic field distributions in the dielectric materials due to the current distribution in a PEC as

$$\alpha_{rad} = \left(\frac{\pi}{2}\right)^5 2\left(\frac{\left(1 - \cos^2(\Psi)\right)^2}{\cos(\Psi)}\right)\frac{(s+2w)^2\varepsilon_r^{3/2}}{c^3 K\left(\sqrt{1-k^2}\right)K(k)}f^3, \quad (3)$$

where $s$ and $w$ are the CPW line and slot width, $k = s/(s+2w)$, and $K(k)$ is the complete elliptical integral of the first kind. It can be seen in Eq. (3) that the magnitude of radiation loss is strongly dependent on $\Psi$, which is given by the discrepancy of the dielectric constants,

$$\cos(\Psi) = \frac{\sqrt{\varepsilon_{eff}(f)}}{\sqrt{\varepsilon_r}}. \quad (4)$$

For a PEC CPW, this ratio is only dependent on the substrate and independent of the conductor properties. However, in a superconducting CPW, the kinetic inductance per unit length $L_k$ due to the inertia of Cooper pairs needs to be taken into account, changing Eq. (1) to

$$\varepsilon_{eff} = c^2(L_g + L_k)C, \quad (5)$$

where the transmission line inductance is the sum of its kinetic inductance and geometric inductance $L_g$.

Conceptually, using a CPW with high $L_k$ leads to a suppression of the radiation loss, as the radiative angle $\Psi$ is reduced. If $L_k$ is sufficiently large to obtain $\varepsilon_{eff} \geq \varepsilon_r$, the radiative shockwave does not form as the phase velocity of the CPW line is slower than that in the substrate, resulting in theoretically zero radiation loss. The kinetic inductance Lk increases with the film normal state sheet resistance, a reduced film thickness (in the regime of thin films compared to the penetration depth), and with the reducing linewidth. A CPW of a 100 nm NbTiN film of 6 $\mu$m wide in total will fulfill the condition that $\varepsilon_{eff} > \varepsilon_r$ (see the supplementary material). Another method is to use a CPW fabricated on a vanishingly thin dielectric membrane, which can be approximated as a free standing CPW and, therefore, does not radiate.

Measuring the radiation loss of a superconducting CPW at sub-millimeter wavelengths requires a highly sensitive device, capable of measuring a loss tangent $\tan\delta < 10^{-3}$. For this purpose, we design a chip with a Fabry–Pérot resonator at its core, as shown in the schematic of Fig. 2(a). A similar device has been used by Göppl et al.[8] at microwave frequencies.

The Fabry–Pérot (FP) resonator is a single CPW line terminated by two identical couplers on either end, with the resonance condition

$$F_n = n\frac{c}{2L_{FP}\sqrt{\varepsilon_{eff}}}, \quad (6)$$

where $\varepsilon_{eff}$ is the effective dielectric constant of the CPW, $L_{FP}$ is the resonator length, and $n$ is the mode number. Transmission through the resonator can be described as a series of Lorentzian peaks, where each peak has a loaded Quality factor $Q_L$ given by the resonance frequency and FWHM (full width at half maximum),

$$Q_L = \frac{F_n}{\text{FWHM}_n}. \quad (7)$$

The loaded Q-factor is a measure of the power loss per cycle, which can be separated in its two primary components,

$$\frac{1}{Q_L} = \frac{1}{Q_c} + \frac{1}{Q_i}. \quad (8)$$

First, $Q_c$ is the power leakage through the two couplers,

$$Q_c(n) = \frac{n\pi}{|S_{2'1'}|^2}, \quad (9)$$
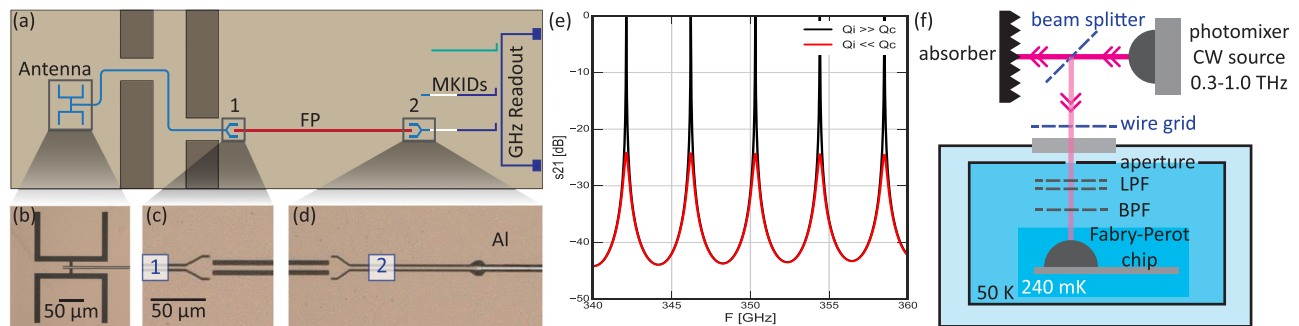


**FIG. 2.** (a) Chip schematic. (b) Picture of the antenna. (c) Picture of the first coupler. (d) Picture of the second coupler, including the transition to the Aluminum section of the MKID. (e) Simulated Fabry–Pérot transmission. (f) Experimental setup schematic. The filterstack consists of Low-pass filters (LPF) and a bandpass filter (BPF). The aperture plane is at the 50 K window, and a polarizing wire grid is located outside the cryostat.

where $|S_{2'1'}|^2$ is the transmission through a single coupler with ports $1'$ and $2'$ (see the supplementary material). Second, the internal losses are described by $Q_i$, which is defined as

$$Q_i = \frac{\beta}{2\alpha}, \qquad (10)$$

with the propagation constant $\beta = 2\pi/\lambda$ and the loss factor $\alpha$, where $[\alpha] = \mathrm{Np/m}$. The loss inside the resonator is given by the combination of Ohmic loss ($Q_{i,ohm}$), dielectric loss ($Q_{i,diel}$), and radiation loss of the CPW ($Q_{i,rad}$), as well as radiation loss at the coupler ($Q_{i,coup}$),

$$\frac{1}{Q_i} = \frac{1}{Q_{i,ohm}} + \frac{1}{Q_{i,diel}} + \frac{1}{Q_{i,rad}} + \frac{1}{Q_{i,coup}}. \qquad (11)$$

Since $Q_L$ is the measured variable, a precise measurement of $Q_i$ requires the exact knowledge of $Q_c$, which is experimentally difficult due to fabrication constraints. Therefore, measurements in the internal loss dominated regime of $Q_c > Q_i$ are preferred since then $Q_L \approx Q_i$ [see Eq. (8)]. However, $Q_c$ cannot be increased arbitrarily, as this will reduce the Lorentzian peak height according to

$$|S_{21}|_{max} = \frac{Q_L}{Q_c}, \qquad (12)$$

as shown in Fig. 2(e). Additionally, we use in the experiments a source with limited frequency resolution, limiting the design range of $Q_c$ values as well. Taking these considerations into account, all chips discussed in this paper are designed in Sonnet[9] to have $Q_c^{design} = 2.7 \times 10^4$ at 350 GHz (see the supplementary material). The center frequency of 350 GHz is chosen based on the available experimental setup.

In order to measure the CPW radiation loss dependency on $\varepsilon_{eff}$ in Eqs. (3) and (4), four chips are designed with varying linewidths $w$ and slotwidths $s$ of the Fabry–Pérot lines as given in Table I. All chips are fabricated on a single 350 $\mu$m thick Sapphire wafer, ensuring common film properties across the chips. The 100 nm NbTiN film is deposited directly on the Sapphire using reactive sputtering of a NbTi target in a Nitrogen–Argon atmosphere.[10] The details on the fabrication can be found in the study by Endo et al.,[11] which follows the same route as this paper.

The measured line geometry is determined via SEM (Scanning Electron Microscope) inspection and deviates slightly due to over-etch in the fabrication process. Using the surface inductance of $L_s = 1.03$ pH at 350 GHz calculated from the measured film parameters ($T_c = 14.7$ K, $\rho_N = 102\ \mu\Omega$cm) and the known parameters of the C-plane Sapphire substrate ($\varepsilon_r^C = 11.5$; $\varepsilon_r^{AB} = 9.3$), we obtain the measured values of $\varepsilon_{eff}$ at 350 GHz given

**TABLE I.** Designed and measured slot width $w$ and linewidth $s$ and resulting $\varepsilon_{eff}$ for each chip's Fabry–Pérot resonator.

| | $w_d = s_d\ [\mu m]$ | $s_{meas}\ [\mu m]$ | $w_{meas}\ [\mu m]$ | $\varepsilon_{eff}$ |
|---|---|---|---|---|
| Chip I | 2 | 1.95 | 2.15 | 13.1 |
| Chip II | 3 | 2.95 | 3.15 | 10.9 |
| Chip III | 4 | 3.95 | 4.15 | 9.5 |
| Chip IV | 5 | 4.95 | 5.15 | 9.0 |

in Table I. NbTiN parameters are measured on a test sample close to the FP resonators to eliminate effects of spatial variations in the NbTiN properties.[10] The resonator length is $L_{FP} = 10$ mm, corresponding to mode numbers in the range of 60–90 for the four chips.

A first estimate of the radiation loss, naively using Eq. (5) in Eq. (3) to account for the kinetic inductance, ranges from $Q_i = 5.6 \times 10^3$ for the 5 $\mu$m line to $Q_i = 5.4 \times 10^6$ for the 3 $\mu$m line; for the 2 $\mu$m line, the equation diverges.

Using Mattis–Bardeen theory,[12] we can estimate the Ohmic losses to be multiple orders of magnitude higher than the stated loss, which means that radiation loss dominates for $w = s > 2\ \mu$m. It has been shown previously that highly disordered superconductors start to deviate from Mattis–Bardeen theory[13] for high frequencies ($f > 0.3\Delta$) and high normal-state resistivity ($\rho_N > 100\ \mu\Omega$ cm). However, both the frequency range of this experiment and the NbTiN film resistivity are at the lower limit, and only a minimal deviation is expected.

In order to drive the FP resonator, one coupler (port 1) is connected via a CPW with $w = 2\ \mu$m and $s = 2\ \mu$m to a double-slot antenna, centered at 350 GHz. The other coupler (port 2) is directly attached to the shorter end of a Microwave Kinetic Inductance Detector (MKID), which is a $\lambda/4$ resonator with $F_{res} \approx 6.5$ GHz based on the hybrid CPW design introduced by Janssen et al.[14] In the MKID, a 1.5 mm long, narrow hybrid CPW with a NbTiN ground plane and an Al ($\Delta_{Al} \approx 90$ GHz $T_c = 1.28$ K) centerline follows directly after a NbTiN coupler section as shown in [Fig. 2(d)]. Incoming THz radiation is absorbed in the low bandgap Al line, thereby creating quasiparticles, which changes the kinetic inductance of the film. This causes a frequency shift of the MKID resonator, which is read out with the SPACEKID microwave readout.[15]

Additional MKIDs, which are not coupled to the Fabry–Pérot and hereafter referred to as blind MKIDs, are placed on the chip as reference detectors. A microwave resonator with the same CPW geometry as the FP resonator is also added [green line in Fig. 2(a)]. Sampling the full FP transmission requires a measurement with a dynamic range of $\approx$50 dB [see Fig. 2(e)]. In order to reduce stray light reaching the MKIDs, the copper holder in which the chip is placed contains a labyrinth structure, as shown in Fig. 2(a), separating the chips that exposed the antenna section from the dark Fabry–Pérot section. Additionally, a low-Tc backside layer of beta-Ta is deposited on the chip backside and acts as a stray light absorber.[16]

In the experiment, we mount an 8 mm Si lens on the chip backside, centered on the antenna, and place both in the Cu sample holder. This is placed on the cold stage of a He-3/He-4 sorption cooler,[17] as shown in Fig. 2(f), operating at $T \approx 250$ mK. A commercial photomixer continuous wave (CW) source[18] is positioned at room temperature and coupled into the cryostat via a beam splitter to reduce the incoming power and avoid saturation of the MKIDs. The source emits a linear polarized, single frequency signal that is tunable in the range of 0.1...1.2 THz with a minimum step size of $\sim$10 MHz and an absolute frequency accuracy of $<$2 GHz. A bandpass filter stack centered at $F_c = 346$ GHz and $>$20 dB out-of-band suppression is located in the cryostat with a polarizing wire grid mounted on the vacuum window.

The FP transmission of the four chips is measured by sweeping the CW source from 310 GHz to 380 GHz in 10 MHz steps with an integration time of 1 s and detecting the resulting MKID response. An electrical on/off modulation of the CW source at $f_{mod} = 11.97$ Hz is employed to avoid 1/f noise. As the CW output power and beam shape

are not well known, the absolute coupling strength to the MKID is not measured and the given responses are relative to the noise floor. However, the detector linearity in the measurement range was confirmed by measuring at various CW powers and retrieving identical results for the FP peak shapes.
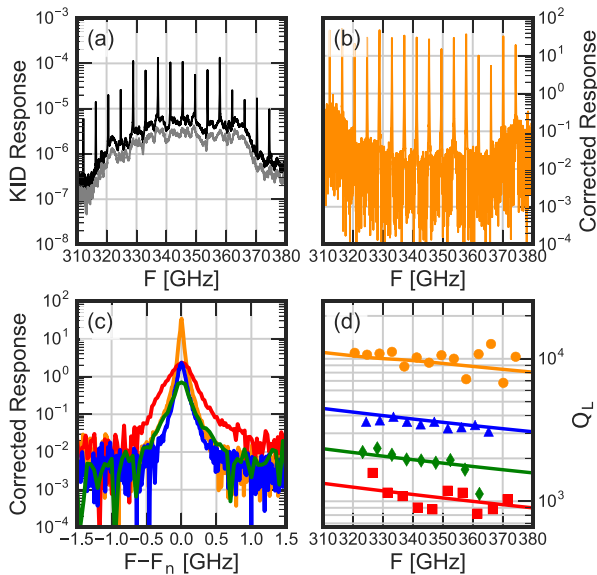
The resulting response $S_D$ of the FP-coupled MKID, shown in Fig. 3(a) exemplarily for chip I, clearly shows the expected regular spaced peaks of the FP resonator combined with a strongly frequency dependent baseline. The blind MKID spectrum $S_B$ shows the same baseline but with a frequency independent offset $O$ compared to $S_D$. As the same baseline is present in both detectors, we attribute it to CW power directly coupling to the MKIDs. Its frequency dependence is given by inherent fluctuations of the CW source combined with the bandpass filter transmission, both of which are also present in the Fabry–Pérot transmission, while the constant offset is due to the difference in MKID responsivity. We retrieve the corrected FP transmission $S_{FP}$ shown in Fig. 3(b) using

$$S_{FP} = S_D/S_B - O, \qquad (13)$$

where $O$ is determined in the regions between FP peaks, where $S_D$ is dominated by the direct coupling.

A comparison between the FP peaks of the 4 chips [see Fig. 3(c)] shows sharper and higher peaks for narrower CPWs. This already indicates lower losses for the narrow CPWs, as the experiments were designed for the $Q_i$-limited regime ($Q_L \approx Q_i$). The peak height difference for chip IV is due to the use of a different aperture, which only affects the direct CW coupling and not the resonance Q factor.

In order to obtain $Q_L$, the individual peaks are fitted with a Lorentzian function
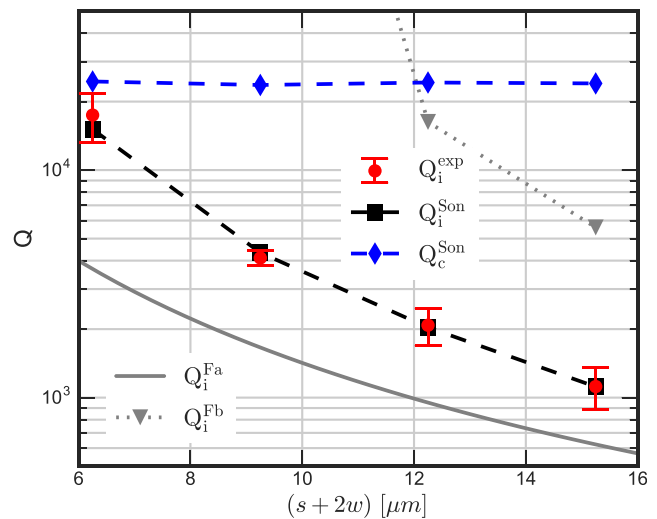
$$L_n(F) = I \frac{Q_{L,n}^2}{Q_{L,n}^2 + 4\left(\frac{F - F_n}{F_n}\right)^2} + O_L, \qquad (14)$$

with peak height $I$ and offset $O_L$, and the fit results are substituted into Eq. (7). The fitted $Q_L$ is shown in Fig. 3(d) as dots and compared to simulations shown by lines.

The simulations are carried out in Sonnet (see the supplementary material) and are based on the measured CPW geometry and NbTiN properties as discussed previously. An excellent agreement with the measured data is found by including the coupling strength $S_{2'1'}$ and radiation loss of the CPW in these simulations. The observed frequency dependence of $Q_L$ is due to both the changing coupling strength and line loss $\alpha \propto f^3$, while the oscillation in measured $Q_L$ can be explained qualitatively by a standing wave before the first FP coupler with a resonance length $L_{sw} > L_{FP}$.

In order to extract the internal loss from the measured $Q_L$, $Q_c$ must be known. While it is, in principle, possible to measure $Q_c$ directly using the analysis in Fig. 2(e), this requires a dynamic range >50 dB or an absolute calibration of $S_{21}$ at the resonance peaks, both of which are not possible in our experimental system. Therefore, we use the Sonnet simulations of the coupler to obtain $Q_c$.

We then average over all peaks in the frequency range to retrieve $Q_i^{exp}$ at 350 GHz, shown in Fig. 4, which is in excellent agreement with the Sonnet simulations of the CPW radiation loss. It is significantly higher than the analytical solution $Q_i^{Fa}$ for the case of a PEC using Eq. (3), with the difference increasing for narrower lines up to a factor of 4. However, it is also significantly lower than the naive approach of substituting the superconducting $\varepsilon_{eff}$ of Eq. (5) into Eq. (3), resulting in $Q_i^{Fb}$. All four CPW geometries are within the validity range for Eq. (3), but as the derivation of Eq. (3) is based on a planar PEC geometry and does not take a superconductor into account, it is not surprising that both these approaches fail. For $Q_i^{Fa}$, the phase velocity change due to the kinetic inductance is completely neglected, while the naive



**FIG. 3.** (a) Measured spectrum for chip I of the Fabry–Pérot coupled MKID (*black*) and the blind MKID (*gray*). (b) Corrected spectrum of the FP coupled MKID of chip I. (c) Example peaks of the corrected spectra of each chip (I: *orange*; II: *blue*; III: *green*; IV: *red*) (d) Measured $Q_L$ for all chips indicated by symbols and simulated $Q_{L,sim}$ by lines, using the previously defined color scheme.



**FIG. 4.** Measured $Q_i^{exp}$ compared to sonnet simulations for internal loss $Q_i^{Son}$ and coupling strength $Q_c^{chip}$, as well as analytical solutions for a PEC CPW $Q_i^{Fa}$ and superconducting CPW $Q_i^{Fb}$.

inclusion of $L_k$ in $\varepsilon_{eff}$ for $Q_i^{Fb}$, which is correct for phase velocity considerations, does not take into account the actual field distribution in the dielectric. The $Q_i$ value of the NbTiN microwave resonator located on each of the chips is measured to be $\approx 2 \times 10^6$, which is consistent with previous experiments[19] and indicates no issues with film quality.

In addition to the quantitative disagreement between the experiment and the analytical solution, we find a non-zero loss for chip I where we expect no radiation loss according to the shockwave model. As $\varepsilon_{eff} > \varepsilon_r$ is a fundamental argument against radiation loss due to a shockwave, a different mechanism must be considered. Radiation loss, due to the strong fields at the open ended couplers, was found to have a negligible contribution in sonnet simulations with $Q \approx 10^5$ (see the supplementary material). Dielectric losses due to the crystalline sapphire substrate are expected to be negligible and can be excluded due to the high $Q_i$ of the microwave resonator. Ohmic losses due to disorder effects in the NbTiN film are expected to be much smaller than those observed and are not compatible with the measured width dependence. Additionally, none of these losses are included in the simulation for $Q_i^{son}$, where we find a quantitative agreement with the measurements. Due to this excellent agreement, we speculate that we are limited by a different loss mechanism, most likely due to the fundamentally unconfined nature of the CPW mode.

In conclusion, we have designed, fabricated, and measured superconducting on-chip CPW Fabry–Pérot resonators with high kinetic inductance NbTiN ($L_s = 1.03/\text{pH}$) and multiple line dimensions at frequencies from 320 to 380 GHz. We find a linewidth dependence for the internal loss $Q_i$, with values of $(1.1 \pm 0.2) \times 10^3$ for a total linewidth of 15.25 $\mu$m to $(1.7 \pm 0.4) \times 10^4$ for 6.25 $\mu$m, corresponding to $\alpha = 0.007$ dB/mm and $\alpha = 0.09$ dB/mm, respectively. The measured loss is in quantitative agreement with simulations of the radiation loss using Sonnet. However, the analytical solution reported by Frankel et al.[7] is not valid in the regime of high-kinetic inductance superconductors, underestimating the CPW loss when $\varepsilon_{eff} \approx \varepsilon_r$.

Furthermore, we show that the on-chip Fabry–Pérot resonator provides a sensitive and highly flexible method for high-$Q_i$ transmission line loss measurements at submillimeter wavelengths. Extensions to other transmission line types, such as microstrips, can be easily achieved by modifying the resonator line and couplers, while the antenna can be exchanged to fit the required frequency range. Further optimization in the quasi-optical path and chip design are viable paths to improve the dynamic range and reduce effects from standing waves. For measurements of narrower lines where even lower losses are expected, a THz source with higher frequency resolution, such as multipliers, is required.

See the supplementary material for the analytical characterization of a superconducting CPW and a comprehensive discussion of the Sonnet simulations for the Fabry–Pérot resonators.

The data that support the findings of this study are available from the corresponding author upon reasonable request.

## REFERENCES

[1]A. Endo, K. Karatsu, Y. Tamura, T. Oshima, A. Taniguchi, T. Takekoshi, S. Asayama, T. J. L. C. Bakx, S. Bosma, J. Bueno, K. W. Chin, Y. Fujii, K. Fujita, R. Huiting, S. Ikarashi, T. Ishida, S. Ishii, R. Kawabe, T. M. Klapwijk, K. Kohno, A. Kouchi, N. Llombart, J. Maekawa, V. Murugesan, S. Nakatsubo, M. Naruse, K. Ohtawara, A. Pascual Laguna, J. Suzuki, K. Suzuki, D. J. Thoen, T. Tsukagoshi, T. Ueda, P. J. de Visser, P. P. van der Werf, S. J. C. Yates, Y. Yoshimura, O. Yurduseven, and J. J. A. Baselmans, Nat. Astron. **3**, 989 (2019).

[2]G. Cataldo, E. M. Barrentine, B. T. Bulcha, N. Ehsan, L. A. Hess, O. Noroozian, T. R. Stevenson, K. U-Yen, E. J. Wollack, and S. H. Moseley, J. Low Temp. Phys. **193**, 923 (2018).

[3]E. Shirokoff, P. S. Barry, C. M. Bradford, G. Chattopadhyay, P. Day, S. Doyle, S. Hailey-Dunsheath, M. I. Hollister, A. Kovács, C. McKenney, H. G. Leduc, N. Llombart, D. P. Marrone, P. Mauskopf, R. O'Brient, S. Padin, T. Reck, L. J. Swenson, and J. Zmuidzinas, Proc. SPIE **8452**, 84520R (2012).

[4]P. A. R. Ade, R. W. Aikin, D. Barkats, S. J. Benton, C. A. Bischoff, J. J. Bock, J. A. Bonetti, J. A. Brevik, I. Buder, E. Bullock, G. Chattopadhyay, G. Davis, P. K. Day, C. D. Dowell, L. Duband, J. P. Filippini, S. Fliescher, S. R. Golwala, M. Halpern, M. Hasselfield, S. R. Hildebrandt, G. C. Hilton, V. Hristov, H. Hui, K. D. Irwin, W. C. Jones, K. S. Karkare, J. P. Kaufman, B. G. Keating, S. Kefeli, S. A. Kernasovskiy, J. M. Kovac, C. L. Kuo, H. G. LeDuc, E. M. Leitch, N. Llombart, M. Lueker, P. Mason, K. Megerian, L. Moncelsi, C. B. Netterfield, H. T. Nguyen, R. O'Brient, R. W. O. Ogburn IV, A. Orlando, C. Pryke, A. S. Rahlin, C. D. Reintsema, S. Richter, M. C. Runyan, R. Schwarz, C. D. Sheehy, Z. K. Staniszewski, R. V. Sudiwala, G. P. Teply, J. E. Tolan, A. Trangsrud, R. S. Tucker, A. D. Turner, A. G. Vieregg, A. Weber, D. V. Wiebe, P. Wilson, C. L. Wong, K. W. Yoon, and J. Zmuidzinas, Astrophys. J. **812**, 176 (2015).

[5]B. Ho Eom, P. K. Day, H. G. LeDuc, and J. Zmuidzinas, Nat. Phys. **8**, 623 (2012).

[6]J. Gao, A. Vayonakis, O. Noroozian, J. Zmuidzinas, P. Day, and H. Leduc, AIP Conf. Proc. **1185**, 164 (2009).

[7]M. Y. Frankel, S. Gupta, J. A. Valdmanis, and G. A. Mourou, IEEE Trans. Microwave Theory Tech. **39**, 910 (1991).

[8]M. Göppl, A. Fragner, M. Baur, R. Bianchetti, S. Filipp, J. M. Fink, P. J. Leek, G. Puebla, L. Steffen, and A. Wallraff, J. Appl. Phys. **104**, 113904 (2008).

[9]EM User's Manual (Sonnet Software, Inc., Liverpool, NY, 2008).

[10]D. J. Thoen, B. G. C. Bos, E. A. F. Haalebos, T. M. Klapwijk, J. J. A. Baselmans, and A. Endo, IEEE Trans. Appl. Supercond. **27**, 1 (2017).

[11]A. Endo, K. Karatsu, A. P. Laguna, B. Mirzaei, R. Huiting, D. Thoen, V. Murugesan, S. J. C. Yates, J. Bueno, N. V. Marrewijk, S. Bosma, O. Yurduseven, N. Llombart, J. Suzuki, M. Naruse, P. J. de Visser, P. P. van der Werf, T. M. Klapwijk, and J. J. A. Baselmans, J. Astron. Telesc., Instrum., Syst. **5**, 1 (2019).

[12]D. C. Mattis and J. Bardeen, Phys. Rev. **111**, 412 (1958).

[13]E. F. C. Driessen, P. C. J. J. Coumou, R. R. Tromp, P. J. de Visser, and T. M. Klapwijk, Phys. Rev. Lett. **109**, 107003 (2012).

[14]R. M. J. Janssen, J. J. A. Baselmans, A. Endo, L. Ferrari, S. J. C. Yates, A. M. Baryshev, and T. M. Klapwijk, Appl. Phys. Lett. **103**, 203503 (2013).

[15]J. van Rantwijk, M. Grim, D. van Loon, S. Yates, A. Baryshev, and J. Baselmans, IEEE Trans. Microwave Theory Tech. **64**, 1876 (2016).

[16]S. J. C. Yates, A. M. Baryshev, O. Yurduseven, J. Bueno, K. K. Davis, L. Ferrari, W. Jellema, N. Llombart, V. Murugesan, D. J. Thoen, and J. J. A. Baselmans, IEEE Trans. Terahertz Sci. Technol. **7**, 789 (2017).

[17]S. Hähnle, J. Bueno, R. Huiting, S. J. C. Yates, and J. J. A. Baselmans, J. Low Temp. Phys. **193**, 833 (2018).

[18]TERABEAM 1550, TOPTICA Photonics AG. Lochhamer Schlag, Gräfelfing, Germany.

[19]R. Barends, N. Vercruyssen, A. Endo, P. De Visser, T. Zijlstra, T. Klapwijk, P. Diener, S. Yates, and J. Baselmans, Appl. Phys. Lett. **97**, 023508 (2010).